Influence of Model Globular Proteins with Different Isoelectric Points on the Precipitation of Calcium Carbonate

ARTICLE *in* CRYSTAL GROWTH & DESIGN · APRIL 2008

Impact Factor: 4.89 · DOI: 10.1021/cg070512q

CRYSTAL GROWTH & DESIGN
2008
VOL. 8, NO. 5
1495–1502

Influence of Model Globular Proteins with Different Isoelectric Points on the Precipitation of Calcium Carbonate

A. Hernández-Hernández,[†] A. B. Rodríguez-Navarro,[‡] J. Gómez-Morales,*[,†] C. Jiménez-Lopez,[§] Y. Nys,[||] and J. M. García-Ruiz[†]

Laboratorio de Estudios Cristalográficos, IACT (CSIC-UGRA), Edificio Instituto López Neyra. Avda. del Conocimiento, s/n. P.T. Ciencias de la Salud, 18100 Armilla, Granada, Spain, Departamento de Mineralogía y Petrología, Universidad de Granada, Campus Fuentenueva, s/n 18002 Granada, Spain, Departamento de Microbiología, Universidad de Granada, Campus Fuentenueva, 18002 Granada, Spain, and INRA, UR83, Recherches Avicoles, 37380 Nouzilly, France

Received June 6, 2007; Revised Manuscript Received January 4, 2008

ABSTRACT: Several mechanisms have been proposed to explain the interactions between proteins and mineral surfaces formed during biomineralization. To investigate the effect of the surface charge of proteins on calcium carbonate precipitation, a group of globular proteins with similar sizes and molecular weights but with different isoelectric points (iep) has been selected to be added to a $CaCl_2$ solution in free-drift calcium carbonate precipitation experiments. These proteins are lysozyme (Lyz; theoretical iep 9.32), ribonuclease-A (Rib-A; theoretical iep 8.64), myoglobin (Myo; theoretical iep 7.36), and α-lactalbumin (α-La; theoretical iep 4.83). Depending on their isoelectric point and their concentration in the solution, these proteins affected the nucleation, growth, polymorphism and growth morphology of calcium carbonate in different manners, evidencing different types of protein−surface interactions. For the protein with an acidic isoelectric point (α-La), electrostatic interactions were predominant. For proteins with isoelectric points around neutrality or slightly higher (Myo and Rib-A), the foremost interactions were hydrophobic with a certain electrostatic contribution. For the protein with a basic isoelectric point (Lyz), there was not any notable effect on most of the analyzed precipitation properties, evidencing a weaker protein−surface interaction.

1. Introduction

Biomineralization processes involve specific proteins that are released at different times during mineralized tissue formation.[1] These proteins play an important role in the control of the nucleation, polymorphic phase selection, morphology and orientation of crystals.[2a–d] Several mechanisms have been proposed to explain the interactions between proteins and mineral surfaces in formation, among them a combination of electrostatic and stereochemical interactions, as well as geometrical matching.[3a,b] For a better understanding of those mechanisms, it is useful to use systems in which only one kind of interaction predominates.[4] Whether one kind of interaction is predominant will depend on protein characteristics (i.e., size, conformation, surface charge, type of functional groups), on biomineral composition and surface structure, and also on the solution properties, that is, chemical composition and pH. The protein surface charge and the electrical charge developed at the solid−solution interface are both dependent on the isoelectric point (iep) of the proteins, on the point of zero charge of the adsorbent, and also on the solution properties. Therefore such solution properties must have an important role in protein−surface interaction during the formation of biominerals.

The aim of the present study is to determine the effects on calcium carbonate precipitation (i.e., nucleation, growth, polymorphism, and crystal morphology) of a group of globular proteins with similar sizes and molecular weights but with different iep, within a wide range of pH values. This information will be useful to elucidate the kind of protein−surface interactions predominant during the precipitation. The four selected model globular proteins are lysozyme (Lyz; theoretical iep 9.32, MW 14.313 Da), ribonuclease-A (Rib-A; theoretical iep 8.64; MW 13.690 Da), myoglobin (Myo; theoretical iep 7.36; MW 16951 Da), and α-lactalbumin (α-La; theoretical iep 4.83; MW 16.224 Da).[5a,b] They were chosen because their three-dimensional structures and their adsorption behaviors on different substrates are well characterized. Since the $CaCO_3$ precipitation experiments will be performed using a free-drift system containing the protein-bearing calcium solutions, the change in the pH values of such solutions during the course of the experiment will lead to a change in the surface charge of the protein. It was demonstrated by other authors that the surface charge is one of the most relevant parameters responsible for the differences observed in the adsorption behavior of these proteins on different types of hydrophilic and hydrophobic substrates.[5a,6] The novelty of the present work is that protein−mineral interactions are studied under dynamic conditions since the mineral substrates are growing crystals.

2. Materials and Methods

2.1. Experimental Procedures. Certified chemical reagents were used to prepare stock solutions of $CaCl_2$ (Sigma, lot 110K0226) and NH_4HCO_3 (Sigma, lot 78H0114) and of the following commercial proteins: hen egg white lysozyme (Seikagaku lot E98301), bovine pancreatic ribonuclease-A (Sigma lot 9001 99 4), horse skeletal muscle myoglobin (Sigma lot 100684 32 0), and bovine milk α-lactalbumin (Sigma lot 9051 29 0). Lyz is found in the uterine fluid of hens as well as in the eggshell. The possible role of this and other uterine fluid proteins on eggshell calcification is actually under investigation. The function of Rib-A is RNA cleavage in the ruminant pancreas. Myo is classified as transport protein that delivers oxygen and carbon monoxide through the tissues. α-La is synthesized in the mammary gland and is essential for milk production.

Precipitation experiments were carried out by vapor diffusion using the sitting drop crystallization method on a "crystallization mushroom"[7a,b] at 20 °C and 1 atm total pressure. Calcium carbonate precipitated in

* To whom correspondence should be addressed. E-mail address: jaime@lec.csic.es.
[†] Edificio Instituto López Neyra. Avda. del Conocimiento.
[‡] Departamento de Mineralogía y Petrología, Universidad de Granada.
[§] Departamento de Microbiología, Universidad de Granada.
[||] Recherches Avicoles.

10.1021/cg070512q CCC: $40.75
Published on Web 04/11/2008

Table 1. $CaCO_3$ Precipitation in the Presence of Four Model Proteins (Lyz, Rib-A, Myo, and α-La) Using As Control Conditions 20 mM $CaCl_2$, 10 mM NH_4HCO_3, and $T = 20 \pm 1$ °C

				% $CaCO_3$ polymorphs						
run	[protein], μg/mL	TNC[a]	t_i[b] (min)	C_R[c]	C_S[d]	A[e]	V[f]	L (μm) ± SE[g]	pH_i[h]	pH_f[i]
control	0	40–60	~600	63		15	22	92 ± 6	5.3	7.1
Lyz-1	16	49	500	55		21	24	76 ± 6		
Lyz-2	128	52		84		11	5	65 ± 5 and 113 ± 14	5.8	7.2
Lyz-3	512	60	700	84		10	6	68 ± 5 and 113 ± 8		
Lyz-4	2000	41	1400	61		21	18	57 ± 10 and 116 ± 8	6.1	7.0
Rib-A-1	16	43	1080	46	0	16	38	140 ± 9 and 288 ± 32	4.9	7.2
Rib-A-2	128	9	1500	44	13	0	43	130 ± 8 and 160 ± 33	4.6	7.3
Rib-A-3	512	3	1800	26	58	0	16	80 ± 17 and 260 ± 33	4.3	7.5
Rib-A-4	2000	0		0	0	0	0		4.1	7.8
Myo-1	16	38	1020	64	8	12	16	95 ± 9 and 280 ± 20	5.3	7.1
Myo-2	128	36	1320	90	6	0	4	80 ± 6 and 200 ± 15	5.7	7.2
Myo-3	512	11	1300	100		0	0	60 ± 18 and 300 ± 25	6.0	7.5
Myo-4	2000	0		0		0	0		6.5	7.8
α-La-1	16	123	÷500–1000	68		0	32	50 ± 8 and 100 ± 11	5.5	7.3
α-La-2	128	169	~1000	95		0	5	77 ± 4 and 100 ± 4	5.6	7.2
α-La-3	512	162		99		0	1	75 ± 3 and 85 ± 5	5.8	7.3
α-La-4	2000	0		0		0	0		6.0	7.5

[a] Total number of crystals. [b] Induction time for the nucleation. [c] Rhombohedral calcite. [d] Spherical calcite. [e] Aragonite. [f] Vaterite. [g] L = average size; SE = standard error. [h] Initial pH in the drops. [i] Final pH in the drops.

drops containing 40 μL of a $CaCl_2$ solution (20 mM), whose pH was raised by the diffusion of NH_3 gas released by an underlying NH_4HCO_3 solution (10 mM). These control conditions were selected so that the total number of crystals precipitated (TNC) was small enough to be easily counted yet great enough to have good statistics and so that the size of crystals was optimal. Also, under these conditions, the polymorphs calcite, vaterite, and aragonite precipitated in such proportions as to make noticeable any effect of the tested proteins on their relative abundances.[7a] Normally, after several runs using these reagent concentrations, the TNC was around 40–60, with 60–63% calcite, 15–20% aragonite, and 20–22% vaterite. In the protein-bearing experiments, the concentration of the $CaCl_2$ solution was kept constant at 20 mM while the concentrations of protein (0, 16, 128, 512 and 2000 μg/ml) were varied. This $CaCl_2$ solution with varying protein concentration is referred to here as the mother solution. To carry out the experiment, a drop of 40 μL of the mother solution was poured on each one of the ten microbridges already placed inside the crystallization mushroom. A volume of 3 mL of the NH_4HCO_3 solution (10 mM) was poured into the bottom container of the mushroom. The system was then closed and sealed with silicon grease. Three runs were carried out at each concentration to test for reproducibility. Experiments were finished after 48 h, the chambers were opened, and both solution and solid were withdrawn from the microbridges for chemical and morphological analyses.

2.2. Analytical Procedures. The pH value of the mother solutions was determined before and after each experiment using a pH electrode (Titan model, Sentron). Based on repeated measurements, the analytical error was estimated to be ±0.05. The concentrations of Lyz, Rib-A, and α-La in the mother solution were measured by the Layne method[8] using a Varian Cary UV–Vis spectrometer at a wavelength of 280 nm, while the concentration of Myo was determined by the Bradford method.[9] The time elapsed from the moment of closing the reactor until the appearance of the first precipitate in the microbridges (referred to here as induction time, t_i), the TNC, and the identification of the polymorphic phases were all determined using an optical microscope (SZH10 Olympus, 14×), based on characteristic morphologies of crystals associated with each phase. The errors for t_i and TNC were estimated to be ±5% and ±1%, respectively. A univocal relationship between morphology and crystalline phase in the absence of proteins was established in a previous study.[7a] In case of ambiguity, the mineralogical composition of crystals was confirmed by X-ray diffraction using Cu Kα radiation (XRD; D-5000 Siemens) at a grazing angle of 1°. At the end of each run, the precipitate was harvested from the microbridges having been previously rinsed ten times with deionized Milli-Q water, dried at room temperature, and finally coated with gold and inspected with a field emission scanning electron microscope (FESEM, Gemini-1530). Calcite crystal forms were indexed based on the symmetry of crystal faces and by comparing them with a calcite morphological model built with Shape v7.2.1 (Shape Software, Kingsport, TN).

Because of the small number of crystals precipitated in each drop, it was not possible to measure the precipitated mass by weighing crystals with accuracy. Therefore this parameter was roughly estimated using the number and phase of crystals, their average length L from field emission scanning electron microscopy (FESEM) pictures, and the density of either calcite (2.71 g/cm^3), vaterite (2.54 g/cm^3), or aragonite (2.93 g/cm^3) depending on the particular crystalline phase precipitated, to convert volume to precipitated mass. In previous references,[10a,b] a similar method was applied. In the present work, cubes and spheres (calcite), spheres and platelets (vaterite), and spheres and cylinders (aragonite) were considered as the most suitable simple geometrical models, despite the great morphological variety of the crystals obtained. The shape factors of these geometries were taken from the literature.[10c]

Finally, the exposed ionizable amino acids at the surface of the four proteins were identified using the program AREAIMOL from the CCP4 program suite[11] based on Protein Data Bank (PDB) coordinates of their corresponding crystalline structures (Lyz,[12a] Rib-A,[12b] Myo,[12c] and α-La[12d]).

3. Results

3.1. Solution pH. The pH of the solution increased from 5.3 to 7.1 during a representative control experiment (protein-free; Table 2). The increment occurred primarily within the first 1.5 h. Thereafter, increases in pH became slower and the pH stabilized at 7.1. The presence of protein varied the initial pH of the mother solution. Thus, Lyz, Myo, and α-La increased the initial pH. This increase was higher as the protein concentration increased. In contrast, the trend in the pH values of solutions containing Rib-A was the opposite. The initial pH was lower than in the control experiment and decreased as the concentration increased. At the end of the experiment, pH values in protein-bearing experiments were generally similar to or higher than those in the (protein-free) control experiment.

The proteins affected the precipitation of $CaCO_3$ at different levels, that is, nucleation (t_i, TNC), growth (crystal dimensions and mass of crystals), polymorphism, and crystal morphology. Next we describe these effects in detail.

3.2. Effects of Proteins on Nucleation. The influence of proteins on $CaCO_3$ nucleation is illustrated in Figure 1 and Table 1. Moreover, Table 1 summarizes all relevant parameters of $CaCO_3$ precipitation using both protein-free (control) and protein-bearing solutions, including TNC, t_i, and the percentage of polymorphs calcite, vaterite, and aragonite.

The α-La at low concentrations of 16, 128, and 512 μg/mL promoted a very intense nucleation, as deduced from the high

Table 2. Physicochemical Properties of the Model Proteins Hen Egg-White Lysozyme (Lyz), Bovine Pancreatic Ribonuclease-A (Rib-A), Horse Skeletal Muscle Myoglobin (Myo), and Bovine Milk α-Lactalbumin (α-La)

				charged amino acids[a]		% exposed charged amino acid	
protein	theor iep	exptl iep	MW (Da)	positive[b]	negative[c]	positive	negative
Lyz	9.32	11.35[15a]	14313	Lys1, Arg5, Lys13, Arg14, **His15**, Arg21, **Lys33**, Arg45, Arg61, Arg68, Arg73, **Lys96**, Lys97, Arg112, Arg114, Lys116, Arg125, Arg128	Glu7, Asp18, **Glu35**, Asp48, **Asp52**, **Asp66**, Asp87, Asp101, Asp119	18[d]	10
Rib-A	8.64	9.6[15b]	13690	Lys1, Lys7, Arg10, **His12**, Lys31, Arg33, Lys37, Arg39, **Lys41**, **His48**, Lys61, Lys66, Arg85, Lys91, Lys98, **Lys104**, **His105**, His119	Glu2, Glu9, **Asp14**, Asp38, **Glu49**, Asp53, **Asp83**, Glu86, Glu111, **Asp121**	18[e]	10
Myo	7.36	7.2[15c]	16951	**Lys16**, **His24**, Arg31, His36, Lys42, Lys45, Lys47, His48, Lys50, Lys56, Lys62, Lys63, **His64**, Lys77, Lys78, Lys79, His81, **His82**, Lys87, **His93**, Lys96, **His97**, Lys98, Lys102, His113, His116, Lys118, **His119**, Lys133, **Arg139**, Lys145, Lys147	Asp4, Glu6, Glu18, Asp20, Glu27, Glu38, Glu41, Asp44, Glu52, Glu54, Glu59, **Asp60**, Glu83, Glu85, Glu105, Asp109, Asp122, Asp126, Glu136, **Asp141**, Glu148	32[f]	21
α-La	4.83	4.5[15d]	16224	Lys5, Arg10, Lys13, Lys16, His32, **Lys58**, Lys62, His68, Lys79, Lys93, Lys94, **Lys98**, **His107**, Lys108, Lys114, Lys122	Glu1, Glu7, Glu11, Asp14, **Glu25**, **Asp37**, Asp46, Glu49, **Asp63**, Asp64, Asp78, Asp82, Asp83, Asp84, **Asp87**, **Asp88**, Asp97, Glu113, Asp116, Glu121	16[g]	20

[a] Buried amino acids are shown in bold (surface areas <50 Å^2). [b] Lysine, arginine, and histidine. [c] Glutamate and aspartate. [d] Including 11 arginine. [e] Including four arginine and four histidine. Histidine can have an important effect on pH around neutrality. [f] Including two arginine and 11 histidine. Some histidine are buried and linked to the hemo group. [g] Including one arginine and three histidine.

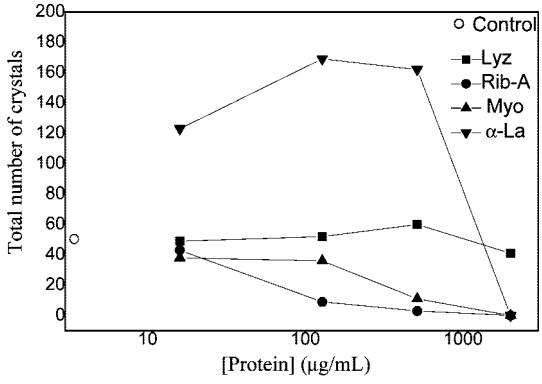

Figure 1. Total number of $CaCO_3$ crystals (TNC) precipitated as a function of the concentration of protein. α-La at 16, 128, and 512 μg/mL favors the nucleation of $CaCO_3$, increasing TNC. Rib-A and Myo slightly decrease TNC when their concentrations are increased from 16 to 512 μg/mL. α-La, Rib-A, and Myo (at 2000 μg/mL) inhibit $CaCO_3$ nucleation completely, decreasing TNC to 0. The effect of Lyz-bearing experiments on TNC is small compared with the control experiments. The open circle represents the control experiment in absence of protein.

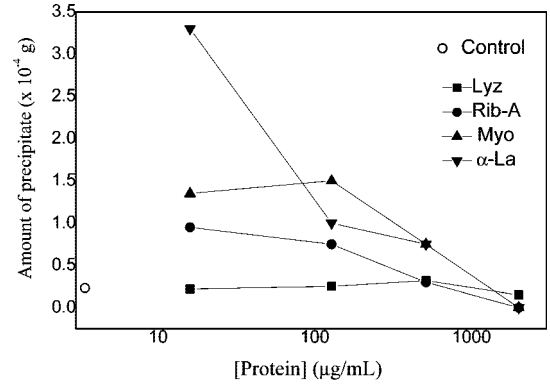

Figure 2. Estimation of the precipitated mass of $CaCO_3$ versus the concentration of protein. α-La, Myo, and Rib-A favor the precipitation of $CaCO_3$ at low concentrations of protein. As the concentration of the three proteins increases to 128 and 512 μg/mL the amount of precipitate gradually decreases, being 0 when the protein concentrations reached 2000 μg/mL. For Lyz-bearing experiments, no noticeable effect in the amount of precipitate with respect to the control experiment is observed in the interval from 16 to 2000 μg/mL.

value of TNC. Rib-A, and to a lesser extent Myo, slightly inhibited the nucleation with respect to the control experiment. When the concentration of these three proteins reached 2000 μg/mL a complete inhibition of $CaCO_3$ nucleation was observed. The effect of Lyz-bearing solutions on $CaCO_3$ nucleation was small in the concentration range from 16 to 2000 μg/mL. It was necessary to increase the Lyz concentration to 5000 μg/mL to reach a complete inhibition of the nucleation.

3.3. Effects of Proteins on Crystal Growth. The results of precipitated mass of $CaCO_3$ and average size of crystals (*L*) are shown in Figure 2 and Table 1.

As it is shown in Figure 2, the precipitation of $CaCO_3$ is favored in α-La-, Myo-, and Rib-A-bearing solutions at low protein concentrations. With these proteins, the estimated mass of precipitate at 16 and 128 μg/mL was higher than that in the control experiment. Further increases in protein concentration led to a decrease of the amount of precipitate, until it reached 0 at 2000 μg/mL protein concentrations. In the case of Lyz, no noticeable change in this parameter was observed with respect to the control experiment in the interval from 16 to 2000 μg/mL. In this case, $CaCO_3$ precipitation was not inhibited completely from mother solutions containing up to 5000 μg/mL.

Although it is a rough estimation, the observed decrease in the amount of precipitate from protein-bearing solutions containing a low protein concentration is worth noting (Figure 2). This decrease occurred following the trend (from acidic to basic proteins) α-La > Myo > RibA > Lyz, thus evidencing a negative correlation of this parameter with the isoelectric point of the model proteins at low protein concentrations.

On the other hand, it is shown in Table 1 that precipitates are polydisperse, with average crystal size *L* (edge length, diameter, or characteristic dimension) varying within a different size range depending on the protein tested. For crystals precipitated in the presence of α-La, *L* falls within the range

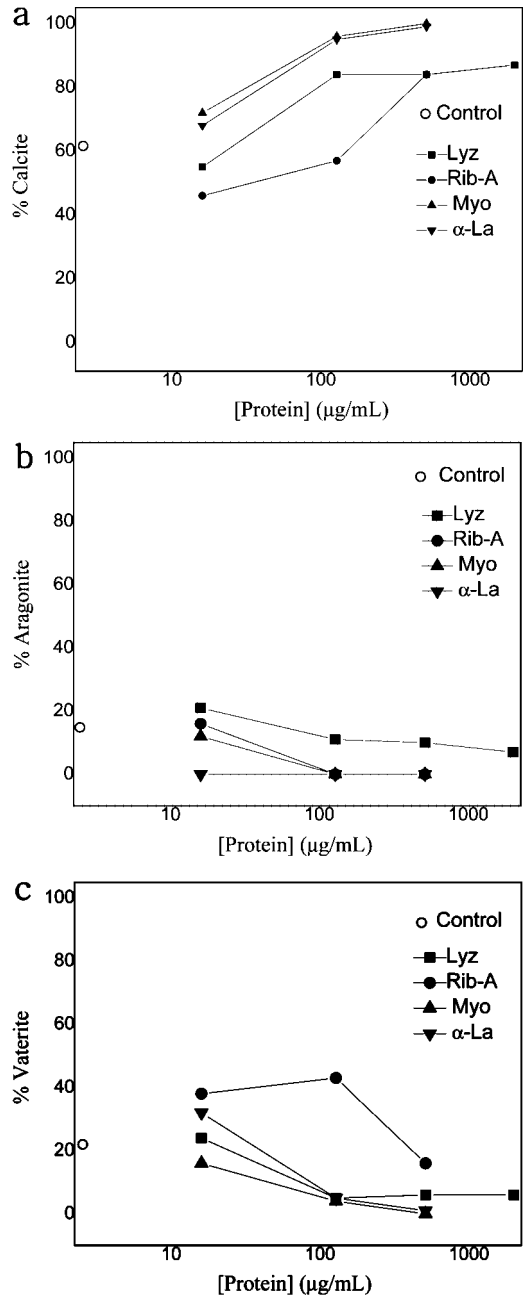

Figure 3. Influence of model globular proteins on the percentage of precipitated $CaCO_3$ polymorphs (a) calcite, (b) aragonite, and (c) vaterite.

50–100 μm, whereas for crystals precipitated in the presence of Myo, Rib-A, and Lyz, L falls within ranges of 60−300 μm), 80−288 μm, and 57−116 μm, respectively. In the control experiment, L was around 92 μm.

3.4. Effects of Proteins on Polymorphism. All model proteins favored the precipitation of calcite over aragonite and vaterite but to different degrees, as deduced from Figure 3a. The percentage of calcite in the precipitates increased from about 45% or 55% up to 85% or 87% in Rib-A- and Lyz-bearing solutions respectively. However, α-La and Myo were more effective in controlling calcite precipitation. Even using low concentrations of these two proteins (128 μg/mL), the relative abundance of calcite reached almost 100%. Interestingly, α-La inhibited aragonite precipitation at very low concentration (16 μg/mL) and also vaterite precipitation at higher concentrations (128 and 512 μg/mL; Figure 3b,c).

3.5. Effects of Proteins on Crystal Morphology. Calcite crystals grown in protein-free solutions (control samples) were obtained in the form of isolated crystals (Figure 4a) with sizes around 90 μm, while aragonite and vaterite were observed as polycrystalline agglomerates (around 100 μm size) formed by smaller primary nanocrystals. Calcite crystals displayed the characteristic rhombohedral habits showing the {104} face (Figure 4a). Aragonite precipitated as needle-like agglomerates and vaterite as hexalobulated leaf-like agglomerates (Figure 4b,c), superstructures similar to those reported by Gehrke et al.[13]

In Lyz-bearing experiments, there was a little effect on the growth morphologies of the polymorphs compared with those from protein-free solutions (see Figure 5a−c). Meanwhile, at concentrations of Rib-A, Myo, and α-La higher than 16 μg/mL, the growth morphology of the calcite phase was modified either by the appearance of new crystal faces (Figure 5d,g,j−l) or, in the cases of Rib-A and Myo (see Figure 5e,h,i), by the formation of rounded/curved polycrystalline agglomerates in the same droplet. Moreover, the biggest agglomerates were usually found at the gas–liquid or gas–liquid−microbridge interfaces. An XRD diagram of those agglomerates collected from different droplets is shown in Figure 6. The diffractogram displays the three characteristic reflections of the calcite phase (JCPDS 5-586), that is, at $2\theta = 29.45°$ ($d = 3.035$ Å), 36.00° (2.495 Å), and 39.45° (2.285 Å).

It is interesting to point out the noticeable effect of Rib-A on calcite morphology. At 512 μg/mL Rib-A, the proportion of rounded calcite (C_S) is twice that of rhombohedral calcite (C_R). Rhombohedral calcite crystals are modified by the expression of new faces stabilized by these proteins. The newly expressed faces are {100} and {110} prismatic forms and {018} negative rhombohedra. The expression of these new faces is especially notable in the presence of α-La (protein concentration of 128 μg/mL) (Figure 5j,k,l).

Based on this, the four globular proteins studied in these experiments modified the growth morphology of precipitated calcite crystals. Among them, Rib-A, Myo, and α-La were more effective than Lyz at producing a more noticeable effect at lower concentrations (Figures 5d,g,j). Finally the most notable effect of these protein concentation on the morphology of the few aragonite and vaterite polymorphs was the crystal size reduction, as well as the size reduction of the constituting primary nanocrystals.

3.6. Surface Ionizable Amino Acids. Table 2 shows the positively (arginine, lysine, histidine) and negatively (aspartate, glutamate) exposed ionizable amino acids for each protein. The number accompanying the amino acid indicates its position in the primary sequence. Most of the ionizable amino acids are placed at the surface of the protein, so the protein surface is constituted by charged and hydrophobic patches with an irregular distribution. Taking into account the aqueous exposition of the ionizable groups, we have used the Expasy ProtParam tool[14] to calculate the theoretical isoelectric points. The experimental isoelectric points are also shown.[15a–d] The differences observed between theoretical and experimental iep arise from the modification of the pK's of the residues owing to the interaction of charged amino acids and the partial burial of charged amino acids.[16]

4. Discussion

Our results evidence the effect of the proteins on calcium carbonate nucleation, growth, phase selection, and morphology.

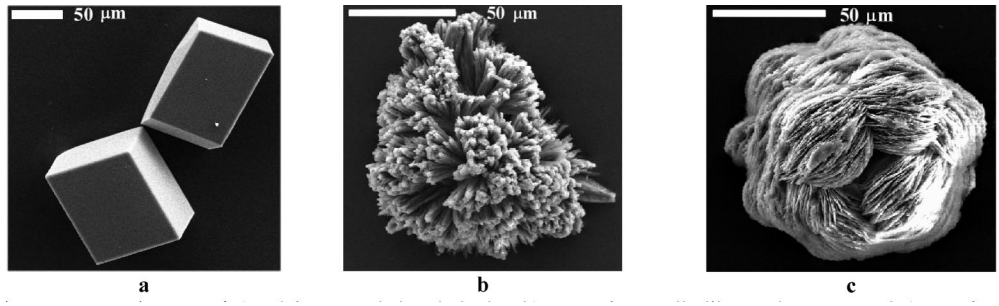

Figure 4. FESEM images of (a) calcite crystal rhombohedra, (b) aragonite needle-like agglomerate, and (c) vaterite leaf-like agglomerate.

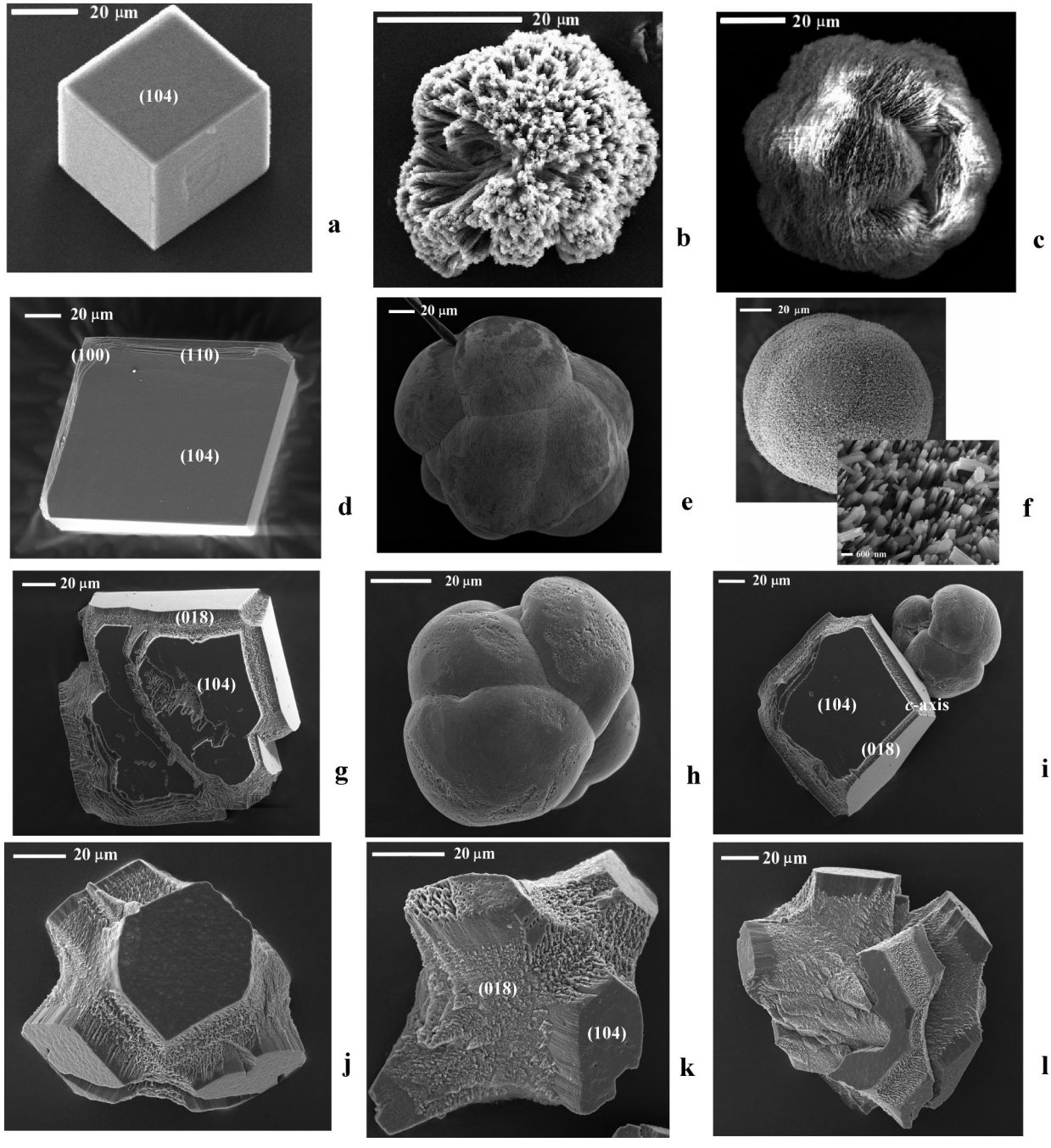

Figure 5. FESEM images of (a) calcite, (b) aragonite, and (c) vaterite with 128 μg/mL Lyz, (d, e) calcite and (f) aragonite with 128 μg/mL Rib-A, (g−i) calcite in presence of 128 μg/mL Myo, and (j−l) calcite in presence of 128 μg/mL α-La.

Also the results suggest that the surface charge and the type and amount of surface ionizable amino acids of the proteins, which determine their iep, have some effect in the above-mentioned factors. Therefore, certain correlations between the

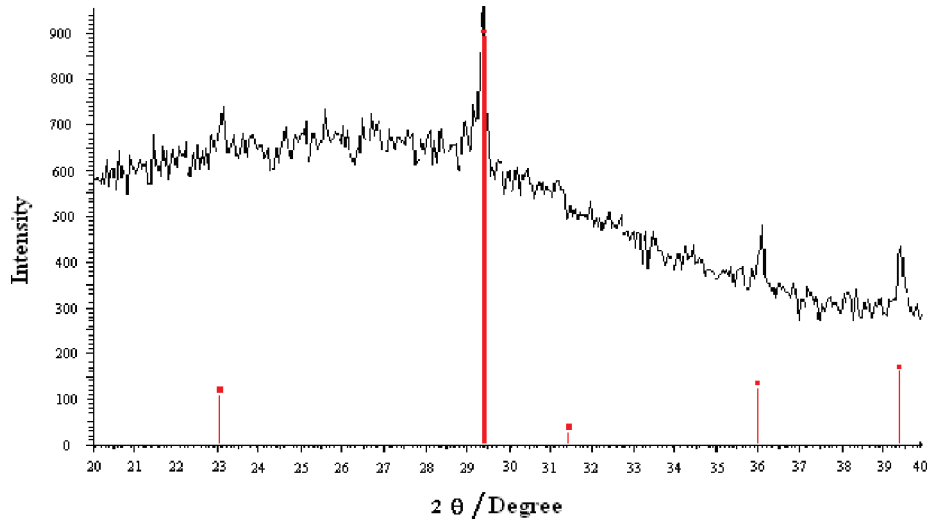

Figure 6. XRD diagram of rounded agglomerates of calcite obtained in Rib-A- and Myo-bearing experiments. The diffractogram displays the three characteristic reflections of the calcite phase (JCPDS 5-586), that is, at $2\theta = 29.45°$ ($d = 3.035$ Å), 36.00° (2.495 Å), and 39.45° (2.285 Å).

isoelectric points of globular proteins and the $CaCO_3$ precipitation parameters can be established.

Modifications of calcium carbonate crystal growth[2a] and dissolution behavior[17] provide insights related to protein−mineral surface interactions. In both cases modifications of the calcite crystals habit are the result of the preferential adsorption of proteins to specific crystal faces, which become expressed as a consequence of the decrease in their growth (or dissolution) rate. Moreover, morphological effects on calcite growth (inhibition of specific crystal faces) vary depending on the nature of the surface charge of the protein.

In Rib-A- and Myo-bearing experiments, which showed the strongest effect on calcite morphology, two types of interaction occurred: (1) a specific protein−surface interaction on planes {110}, {100}, and {001}, which resulted in a morphological effect with the expression of those crystal faces, and (2) a nonspecific interaction, resulting in the precipitation of rounded agglomerates in the same drop. Such a strong nonspecific interaction probably takes place after the nucleation event, once the supercritical nuclei reach nanometric sizes, at the zone of highest supersaturation in the drops. This interaction induces a change in the growth mechanism of calcite from parabolic, which is produced at low to median supersaturation, to an aggregation−agglomeration mechanism, resulting in big (with respect to control size) rounded agglomerates. The aggregation−agglomeration mechanism[18] was proposed to explain the relaxation of residual Gibbs free energy, ΔG, that occurs in highly supersaturated systems after the nucleation event. According to this mechanism the relaxation of residual ΔG takes place by decreasing the total available solid surface (by the aggregation of nanocrystals) rather than by crystal growth.

For a better understanding of the effect of the electrical charges of the globular proteins on the particular growth behavior of the polymorph calcite, it is necessary to consider the calcite surface speciation model proposed by Van Capellen and co-workers.[19] According to this model, the hydrated calcite surface is composed of different types of surface species, these being responsible for the net calcite surface charge in aqueous suspensions. These surface species form by reactions between the neutral surface complexes $<CO_3H°$ and $<CaOH°$ and the soluble species $Ca^{2+}_{(aq)}$, $H^+_{(aq)}$, and $CO_{2(aq)}$ that yield $<CaOH_2^+$, $<CO_3^-$, $<CO_3Ca^+$, $<CaHCO_3°$, $<CaCO_3^-$, $<CO_3H°$, and $<CaOH°$.

It has been demonstrated by using X-ray reflectivity measurements of the calcite{104}−water interface at pH from 6.8 to 12.1 that the proportion of surface species does not vary significantly within this pH range.[20] At the zero point charge of calcite, $pH_{pzc,}$usually between pH 5 and 8, the fraction of positive and negative sites is the same, with a very small proportion of neutral species (less than 2% of $<CaHCO_3°$). An increment in the pH value has the effect of increasing the proportion of neutral species and deprotonation of 18% $<CaOH_2^+$ to yield more neutral $<CaOH°$ species. When a suspension of calcite becomes Ca-rich (by, for instance adding Ca^{2+} ions to the solution), the ξ-potential varies from negative to positive values, which demonstrates a change of the calcite surface charge from negative to slightly positive.[21] Those neutral or basic pH values and a Ca-rich environment closely resemble the solution from which calcite is precipitating in our experiments. Therefore, a slightly positive calcite surface charge with a high proportion of neutral surface species is plausible in our experiments.

Myo and Rib-A are globular proteins with iep intermediate between α-La and Lyz. The iep of Myo is within the range of variation of the solution pH in our experiments, whereas that of Rib-A is slightly above it. In the case of Myo, with 32 positively ionizable surface amino acids, 11 of them are histidines buried or with a surface area less than 50 Å^2, whereas there are 21 negatively ionizable amino acids. Because the pK of histidine is around 6–6.5, at neutral pH they will be ionized and the number of positively and negatively charged surface residues will be the same. Therefore the net charge of this protein (the balance between positively and negatively ionized surface residues) in our experimental conditions is very small or zero. At pH values close to the iep of the protein, the dominant adsorption mechanism on the surface of calcite is a hydrophobic interaction, which favors the dehydration of the proteins by their adsorption to a calcite surface.[22] In the case of Rib-A, 4 of the 18 positively ionizable surface amino acids are arginine and four are histidine, whereas there are 10 negatively ionizable glutamate and aspartate residues. In our experimental conditions of pH, the net charge of Rib-A will be positive but very small; a hydrophobic protein–substrate interaction with an electrostatic contribution is expected. Because of the presence on the protein surface of four arginines with high

hydrophilic power, Rib-A can potentially form H-bonds with the substrate.

The hydrophobic interactions of Myo and Rib-A are unspecific and can occur, under high supersaturation conditions, once the supercritical calcite nuclei reach a certain nanometric size. This mechanism of hydrophobic interaction of proteins with the surface of small crystallites of calcite may account for the formation of the rounded agglomerates of calcite, as detailed above. Further cementation between primary particles is produced by crystal growth.

The hydrophobic interaction being predominant in protein-rich and highly supersaturated environments at pH values close to the isoelectric point of the protein, when conditions change toward low supersaturation or low protein concentrations, calcite crystals grow to micrometric size and the proteins act as impurities. These two mechanisms can act either at the same time in droplets containing Rib-A- or Myo-bearing solutions or successively one after the other. In the first case, the cause is the nonhomogeneity in the concentration of protein and calcium inside the droplets, which leads to zones with different supersaturation (i.e., solution−gas interface versus bulk solution). In the second one, the cause is the strong decrease of the $CaCO_3$ supersaturation and protein concentration that occurs after the first nucleation event. Following this reasoning, it would be plausible to expect a higher proportion of agglomerates by increasing the protein concentration. Indeed, we have increased the concentration of Rib-A up to 8000 μg/mL and obtained only rounded agglomerates.

Lyz has a very different effect on calcium carbonate than that of Myo and Rib-A. Lyz (theoretical iep 9.32, experimental iep 11.35) showed a weaker morphological influence on rhombohedral calcite, compared with that of Myo and Rib-A, even at the highest protein concentration studied. At the pH of our experiments, Lyz has the highest positive net charge of all the proteins tested. Therefore, Lyz has the weakest affinity for the slightly positively charged calcite surface. Therefore, to understand the weak adsorption process and the little effect on most of the analyzed precipitation parameters, it is necessary to look at the surface of the protein. Lyz has 18 positively surface charged amino acids, including 11 arginines, and only 10 negatively charged. Arginine has a high potential to form H-bonds being highly hydrophilic. The high content of arginine is responsible for the high solubility of Lyz in water. Because of the high proportion of surface arginine in this protein and its high capacity to form H-bonds, H-bonding between arginine residues and neutral surface species $<CO_3H°$, $<CaOH°$, and $<CaCO_3°$ could be responsible for the weakly observed Lyz−$CaCO_3$ surface interaction.

On the other hand, α-La does not yield rounded agglomerates of calcite, but it shows a strong effect on nucleation, precipitated mass, polymorph selection, and crystal morphology, even at the lowest protein concentration studied. Moreover, the appearance of new calcite faces is indicative of the existence of a specific interaction. The isoelectric point of α-La is 4.83 (exptl iep 4.5), and therefore, at the pH of our experiments the balance between negatively and positively charged surface residues (Table 2) leads to a negative net surface charge. Such a negative surface charge provides an important interaction with the positively charged calcite surface, increasing protein absorption on the calcite surface. This strong electrostatic interaction must be more specific toward the polar outermost surfaces of the growing crystals than toward the nonpolar stoichiometric ones, as is explained below, inhibiting their growth preferentially. The first types of surfaces are formed by planes of Ca and planes of CO_3 groups. However, the nonpolar surfaces, are formed by equal amounts of Ca and CO_3 groups, such as the {104} plane. Thus, the electrostatic interaction must take place between deprotonized negatively charged $-COO^-$ groups of the proteins and the positively charged $<CO_3Ca^+$ species of the calcite surface.

It is also interesting to comment that the four proteins studied favor calcite precipitation over the other calcium carbonate polymorphs. The capacity that some organisms have to select the polymorphic phase is well-known.[23a,b] There is evidence from many studies that organisms employ specialized organic macromolecules to control calcium carbonate precipitation. For instance, *in vitro* experiments have shown that specific soluble organic macromolecules composing the organic matrix from mollusk shell layers with different mineralogies are able to select the specific polymorphic phase of calcium carbonate.[23a,b] Polymorph selection is achieved by these macromolecules by inhibiting the formation of one polymorph, thus allowing the selection of other polymorph.[23a,b,24] Our results suggest that (1) globular proteins with different isoelectric points specifically inhibit either aragonite or aragonite and vaterite formation and (2) proteins with acidic isoelectric points require low concentrations to inhibit the formation of the above-mentioned polymorphs.

Moreover, our results evidence that the proteins have opposite effects over calcium carbonate precipitation depending on protein concentration, that is, at low concentration, proteins promote calcium carbonate precipitation, while at higher concentration they inhibit it. This effect is particularly evident when using α-La. This ambivalent behavior of proteins is characteristic of crystallization inhibitors that have a strong affinity for target crystal surfaces.[25a,b] At low concentrations of the inhibitors and when there is an excess of material supply for crystal growth, they act as substrates promoting nucleation and favoring precipitation due to stereochemical affinity with the crystal surface.[26] In contrast, at higher concentration of the inhibitors, they bind to the crystal surface growth sites and inhibit precipitation.[27] Furthermore, it has been demonstrated that the effect of the inhibitors increases as they are more negatively charged.[25a,b] Our results are in agreement with these observations.

There are several possible mechanisms by which these proteins could affect calcium carbonate precipitation: (1) Proteins in solution locally raise Ca^{2+} concentrations in those regions close to negatively charged patches on the protein surface[2a,3a] (the ionotropic effect). This creates local areas with higher supersaturation values than those of the bulk solution. Nucleation would be favored in these areas, even when supersaturation in the bulk solution is not the critical supersaturation to produce nucleation. Therefore, proteins act as nucleation centers promoting nucleation and increasing the precipitation rate. The importance of the ionotropic effect increases as the negative charge of proteins increases. Our results are in accordance with this hypothesis, since we observed a trend of increasing precipitated mass of calcium carbonate with more acidic isoelectric point of the proteins; in other words, with more negatively charged proteins. (2) Some of these proteins (i.e., α-La) that have an affinity for calcium and act as chelating agents reduce the available calcium concentration in solution and the effective bulk supersaturation. A reduced amount of Ca exhausts crystal growth and inhibits precipitation of calcium carbonate. (3) Proteins can adsorb to the incipient crystals and block their accessible surfaces, impeding further crystal growth.

According to our results, the ionotropic effect seems to be important only when low concentrations of proteins having an

acidic isoelectric point are used. In contrast, at higher concentrations of all the proteins tested, the chelating effects of proteins or the adsorption of proteins to the growing surface, or both become dominant, inhibiting precipitation (with the exception of Lyz) and suppressing it totally at about 2000 μg/mL.

5. Conclusions

The presence of globular proteins with different isoelectric points controls the precipitation of calcium carbonate at four different levels. First, proteins control nucleation. At low concentrations (16, 128, and 512 μg/mL), α-La favors the nucleation of $CaCO_3$, increasing the number of crystals, while Rib-A and Myo inhibit nucleation. At high concentrations, all three proteins inhibit nucleation. The effect of Lyz on $CaCO_3$ nucleation is small in the concentration range from 16 to 2000 μg/mL. It is necessary to increase the Lyz concentration up to 5000 μg/mL to reach a complete inhibition of $CaCO_3$ nucleation. Second, proteins control crystal growth. At low protein concentration, the combined effect of proteins on nucleation and growth produces a progressive decrease of the precipitated mass of $CaCO_3$ with increasing isoelectric point of the proteins. Third, proteins control polymorphism. The four proteins studied, when used at specific concentrations, favor calcite precipitation over the other polymorphs, aragonite and vaterite. It is possible to completely inhibit either aragonite or aragonite and vaterite precipitation using globular proteins with progressively lower isoelectric points. Finally, proteins control crystal morphology. The effect of proteins on the morphology of calcite crystals is either the appearance of new faces (Rib-A, Myo, and α-La) or the formation of big polycrystalline rounded agglomerates (Rib-A and Myo). There is not an appreciable effect of Lyz on $CaCO_3$ morphology.

Comparative studies like the present one are useful to understand the role of the charge and of the type and amount of ionizable amino acids of proteins on $CaCO_3$ precipitation. Using globular proteins with different iep allows control of $CaCO_3$ precipitation parameters. Our results provide insights in understanding mineral precipitation control in organisms. Further studies of these kinds of mechanisms will be helpful to understand the role of macromolecules in the mineral deposition by biological organisms.

Acknowledgment. This work has been partially financed by the Projects "EggDefence" of the CE VFP, PIE200630I133 of Spanish CSIC, and MAT2006/11701 of the Spanish Ministry of Education and Science. A.H.H., J.G.M., and J.M.G.R. belong to the research team "Factoría de Cristalización" (Consolider-Ingenio 2010). A.H.H. acknowledges a fellowship from CONACYT (México). A.R.N. and C.J.L. acknowledge financial support through the Programa Ramón y Cajal (Spain). Ana Cámara-Artigas is kindly acknowledged for helpful assistance in identifying surface ionizable residues of the proteins and Carlos Ruiz for English revision.

References

(1) Lowestand, H. A.; Weiner, S. *On Biomineralization*; Oxford University Press: New York, 1989.
(2) (a) Addadi, L.; Weiner, S. *Angew. Chem., Int. Ed. Engl.* **1992**, *31*, 153–169. (b) Falini, G.; Albeck, S.; Weiner, S.; Addadi, L. *Science* **1996**, *271*, 67–69. (c) Belcher, A. M.; Hansma, P. K.; Stucky, G. D.; Morse, D. E. *Acta Mater.* **1998**, *46* (3), 733–736. (d) Nys, Y.; Hincke, M. T.; Arias, J. L.; Garcia-Ruiz, J. M.; Solomon, S. E. *Poult. Avian Biol. Rev.* **1999**, *10*, 143–166.
(3) (a) Addadi, L.; Moradian, J.; Shay, E.; Maroudas, N. G.; Weiner, S. A. *Proc. Natl. Acad. Sci. U.S.A.* **1987**, *84*, 2732–2736. (b) Mann, S.; Archibald, D. D.; Didymus, J. M.; Douglas, T.; Heywood, B. R.; Meldrum, F. C.; Reeves, N. J. *Science* **1993**, *261*, 1286–1292.
(4) Rodríguez-Navarro, A.; García-Ruiz, J. M. *Eur. J. Mineral.* **2000**, *12*, 609–614.
(5) (a) Arai, T.; Norde, W. *Colloids Surf.* **1990**, *51*, 17–28. (b) Haynes, A. C.; Norde, W. *Colloids Surf. B: Biointerfaces* **1994**, *2*, 517–566.
(6) Haynes, A. C.; Norde, W. *J. Colloid Interface Sci.* **1994**, *164*, 394–409.
(7) (a) García-Ruiz, J. M.; Hernández-Hernández, M. A.; Gómez-Morales, J. *Ind. Crystal. VDI-Ber. Nr.* **2005**, *1901*, 963–968. (b) Jiménez-López, C.; Rodríguez-Navarro, A.; Domínguez-Vera, J. M.; García-Ruiz, J. M. *Geochim. Cosmochim. Acta* **2003**, *67*, 1667–1676.
(8) Layne, E. *Methods Enzymol.* **1957**, *3*, 447–455.
(9) Bradford, M. M. *Anal. Biochem.* **1976**, *72*, 248–254.
(10) (a) Jiménez-López, C.; Caballero, E.; Huertas, F. J.; Romanek, C. S. *Geochim. Cosmochim. Acta* **2001**, *65* (19), 3219–3231. (b) Romanek, C. S.; Grossman, E. L.; Morse, J. N. *Geochim. Cosmochim. Acta* **1992**, *56, 1*, 419–430. (c) Myerson, A. S. *Handbook of Industrial Crystallization*, 2nd ed.; Butterworth Heinemann: Woburn, MA, 2002.
(11) CCP4: Collaborative Computational Project, Number 4. The CCP4 Suite: Programs for Protein Crystallography; *Acta Crystallogr.* **1994**, *D50*, 760–763.
(12) (a) Wang, J.; Dauter, M.; Alkire, R.; Joachimiak, A.; Dauter, Z. *Acta Crystallogr.* **2007**, *D63*, 1254–1268, PDB ID 2VB1. (b) Chatani, E.; Hayashi, R.; Moriyama, H.; Ueki, T. *Protein Sci.* **2002**, *11*, 72–81, PDB ID 1FS3. (c) Maurus, R.; Overall, C. M.; Bogumil, R.; Luo, Y.; Mauk, A. G.; Smith, M.; Brayer, G. D. *Biochim. Biophys. Acta* **1997**, *1341*, 1–13, PDB ID 1WLA. (d) Chrysina, E. D.; Brew, K.; Acharya, K. R. *J. Biol. Chem.* **2000**, *275*, 37021–37029, PDB ID 1F6S.
(13) Gehrke, N.; Cölfen, H.; Pinna, N.; Antonietti, M.; Nassif, N. *Cryst. Growth Des.* **2005**, *5* (4), 1317–1319.
(14) Gasteiger, E.; Hoogland, C.; Gattiker, A.; Duvaud, S.; Wilkins, M. R.; Appel, R. D.; Bairoch, A.; Protein Identification and Analysis Tools on the ExPASy Server; In *The Proteomics Protocols Handbook*; Walker, J. M., Ed.; Humana Press: Totowa, NJ, 2005; pp 571−607.
(15) (a) Wetter, L. R.; Deutsch, H. F. *J. Biol. Chem.,* **1951**, *192*, 237–242. (b) Schomberg D., Salzmann, M., Eds. *Enzyme Handbook*; Springer-Verlag: Berlin, 1990; Vol *3*, pp 1–3; under E.C. 3.1.27.5. (c) Bhown, A. S. *Handbook of Protein*; A&M Publications: Birmingham, AL, 1990; pp 5–21. (d) Zittle, C. A. *Arch. Biochem. Biophys.* **1956**, *64*, 144–151.
(16) Creighton, T. *Proteins: Structures and Molecular Properties*, 2nd ed.; W. H. Freeman & Co: New York, 1993.
(17) Teng, H. H.; Dove, P. M. *Am. Mineral.* **1997**, *82*, 878–887.
(18) Rodríguez-Clemente, R.; López-Macipe, A.; Gómez-Morales, J.; Torrent-Burgués, J.; Castaño, V. M. J. *Eur. Ceram. Soc.* **1998**, *18*, 1351–1356.
(19) Van Capellen, P.; Cherlet, L.; Stumm, W.; Wersin, P. *Geochim. Cosmochim. Acta* **1993**, *57*, 3505.
(20) Fenter, P.; Geissebühler, P.; DiMasi, E.; Siajer, G.; Sorensen, L. B.; Sturchio, N. C. *Geochim. Cosmochim. Acta* **2000**, *64* (7), 1221.
(21) Cicerone, D. S.; Regazzoni, A. E.; Blesa, M. A. *J. Colloid Interface Sci.* **1992**, *154*, 423.
(22) Haynes, A. C.; Norde, W. *Colloids Surf. B: Biointerfaces* **1994**, *2*, 517–566.
(23) (a) Falini, G.; Albeck, S.; Weiner, S.; Addadi, L. *Science* **1996**, *271*, 67–69. (b) Belcher, A. M.; Wu, X. H.; Christensen, R. J.; Hansma, P. K.; Stucky, G. D.; Morse, D. E. *Nature* **1996**, *381*, 56–58.
(24) Thompson, J. B.; Paloczi, G. T.; Kindt, J. H.; Michenfelder, M.; Smith, B. L.; Stucky, G.; Morse, D. E.; Hansma, P. K. *Biophys. J.* **2000**, *79*, 3307–3312.
(25) (a) Cody, R. D. *J. Sediment. Petrol.* **1991**, *61*, 704–718. (b) Badens, E.; Veesler, S.; Boistelle, R. *J. Cryst. Growth* **1999**, *198*, 704–709.
(26) Lahav, M.; Leiserowitz, L. *J. Phys. (Paris)* **1993**, *D26*, B22–B31.
(27) Black, S. N.; Bromley, L. A.; Cottier, D.; Davey, R. J.; Dobbs, B.; Rout, J. E. *J. Chem. Soc., Faraday Trans.* **1991**, *87*, 3409–3414.

CG070512Q